ISSN (Print) 1226-1750
ISSN (Online) 2233-6656
Journal of Magnetics 22(4), 689-695 (2017) https://doi.org/10.4283/JMAG.2017.22.4.689

Evaluation of Superficial Dosimetry in Postmastectomy Radiotherapy using High-energy Electromagnetic Radiation Treatment

Yong-Min Song[1,2], Byung-Suk Park[1], Byung-Ki Choi[1], Soo-Il Kwon[2], Jun-Chul Chun[2]*, and Jeong-Min Seo[3]

[1]*Department of Radiation Oncology, Samsung Medical Center, Seoul 06351, Republic of Korea*
[2]*Department of Medical Physics, Kyonggi University, Suwon 16227, Republic of Korea*
[3]*Department of Radiologic Science, Daewon University, Jecheon 27135, Republic of Korea*

(Received 22 November 2017, Received in final form 10 December 2017, Accepted 11 December 2017)

The present study evaluated surface and superficial doses delivered by high-energy electromagnetic radiation treatment in patients who received postmastectomy radiotherapy. Computed tomography was performed using an RW3 slab phantom, and hypothetical target volumes were delineated. 6MV electromagnetic radiation beams were generated with five treatment plans: 2-field 3-dimentional conformal radiation therapy, 4-field intensity-modulated radiation therapy, 7-field intensity-modulated radiation therapy, TomoHelical 3-dimentional conformal radiation therapy, and TomoHelical intensity-modulated radiation therapy. Film dosimetry was performed with Gafchromic EBT3 film for dose measurement of high-energy electromagnetic radiation. The dose profile at the surface and superficial regions (1-6 mm depth) of the phantom obtained for each treatment technique. Compared to other techniques, Tomo 3-dimentional conformal radiation therapy had the highest surface dose (47-71 %). The superficial doses of TomoHelical 3-dimentional conformal radiation therapy and TomoHelical intensity-modulated radiation therapy were > 75 %, 80 %, and 90 % of the prescribed dose at 1, 2, and 5 mm depths, respectively. For postmastectomy radiotherapy, TomoHelical 3-dimentional conformal radiation therapy and TomoHelical intensity-modulated radiation therapy had higher surface and superficial doses than linear accelerator-based treatment techniques, with a sufficient dose of ≥ 75 % being delivered to the skin region at depths of 1 mm.

Keywords : mastectomy, high-energy electromagnetic radiation, radiotherapy, superficial dose, gafchromic EBT3 film

1. Introduction

Postmastectomy radiotherapy (PMRT) has been proven to decrease the local recurrence of cancer [1]. According to a report published in 2005, high-energy electromagnetic radiation therapy to the chest wall of patients who underwent complete mastectomy decreased the recurrence rate from 21 % to 7.8 % [2].

Human skin is composed of the epidermis, dermis, and subcutaneous tissue. Since the subcutaneous tissue contains lymphatic vessels that contain potential cancer cells, it is an especially high-risk region of local recurrence [3]. The thickness of the dermal layer in the breast is reportedly approximately 1-3 mm [4], and because this skin region is highly susceptible to local recurrence of cancer after postmastectomy, a sufficient radiation dose (75-90 % of the prescribed dose) is recommended [5].

For PMRT, the linear accelerator (LINAC) used for equipment most commonly as high-energy electromagnetic radiation treatment. The radiation treatment has been developed into intensity-modulated radiation therapy (IMRT), which is performed through 2-dimentional radiation therapy and 3-dimentional conformal radiation therapy (3DCRT). The natural extension of IMRT is arcing modulated high-energy electromagnetic radiation, such as helical tomotherapy. Tomotherapy delivers IMRT with a continuously rotating, helical fan beam using binary multileaf collimators (MLC) [6]. Conventionaly, two-portal tangential high-energy electromagnetic wave (not electron beam) irradiations are used to treat chestwall as 3DCRT, and a bolus is used to increase the dose to the skin region. However, the added bolus application may lead to skin complications such as erythema, desquamation, or moist desquamation, depending on the absorbed dose

*Corresponding author: Tel: +82-31-249-9668
Fax: +82-31-249-8949, e-mail: jcchun@kyonggi.ac.kr

by the skin; hence, the thickness of the bolus and the number of treatment fractions must be considered at each facility [7, 8]. IMRT and tomotherapy, which enable the delivery of a more uniform dose of high-energy electromagnetic radiation to the chest wall while decreasing the dose to the lungs and heart, have been introduced and widely used in clinical settings. In addition, because of its physical properties, tomotherapy delivers a sufficient dose to the skin region without the use of a bolus, and this led to many earlier studies on tomotherapy [9-12].

As outlined previously, a variety of treatment techniques are used for PMRT. However, as the chest wall has a very thin tissue layer and the lungs have a relatively low density, irradiation with a high-energy electromagnetic beam generally presents dosimetric uncertainty for the calculated dose and measured dose [13]. Doses calculated by the treatment planning system are inaccurate in the region of electronic disequilibrium (e.g., the build-up region) [14]. Moreover, the absorbed dose by the skin region in curved body parts such as the chest wall is affected by the treatment technique; thus, accurate evaluation of the superficial dose is necessary [15].

In the present study, the human chest wall was hypothesized to be a water-equivalent phantom, and we used Gafchromic EBT3 film to measure the surface and superficial doses delivered by various breast treatments using high-energy electromagnetic radiation.

2. Subjects and Methods

2.1. Equipment and the phantom

The LINAC uses high-frequency microwave to accelerate electrons in part of wave guide, then allows these electrons to collide with a heavy metal target to producer high-energy electromagnetic radiation. Electromagnetic radiation constitutes the mode of energy as light waves, heat waves, microwaves, ultraviolet rays, x-rays, and γ-rays. Typically, high-energy electromagnetic radiation, such as x-rays, are types of ionizing radiation [16].

In this study, 6EX LINAC (Varian Medical System, Palo Alto, CA, USA) with 60 pairs of MLCs and a tomotherapy (TomoTherapy, Accuray, Sunnyvale, CA, USA) with 64 pairs of MLCs were used as high-energy electromagnetic radiation therapy equipment. Only 6-MV of high-energy electromagnetic beam was generated equally in all the treatment techniques. The dose calculation for treatment planning was performed using Pinnacle3 (version 9.2, Philips Medical Systems, Madison, WI, USA) and tomotherapy software (TomoTherapy® Planning Station 4.2.2.4, Accuray, USA). The IMRT phantom (IBA, Schwarzenbruck, Germany) with dimensions of 33 (width) × 36 (length) × 18 (height) cm^3 was used. The phantom for high-energy electromagnetic radiation dosimetry was made of RW3 with a density of 1.045 g/cm^3 (Fig. 1).

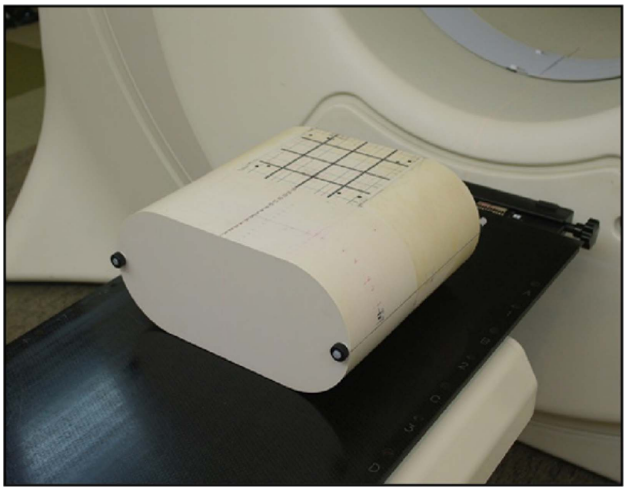

Fig. 1. (Color online) Water-equivalent phantom measuring 36 cm (length) × 33 cm (width) × 18 cm (height).

2.2. Treatment planning

Computed tomography(CT) imaging (LightSpeed, GE Healthcare, Milwaukee, WI, USA) was acquired using a phantom with a thickness of 2.5 mm. The treatment planning system was used on the acquired cross-sectional images for contour of the hypothetical chest wall to a thickness of 2 cm, and a hypothetical clinical target volume and normal tissues were delineated. Considering the patient's movement and set-up error, the planning target volume (PTV) was generated with an error margin of 5 mm in all directions, except in the superficial region. As it is uncertain whether build-up in the treatment planning system occurss due to high energy of electromagnetic wave in the superficial region, the PTV was delineated in the superficial region 5 mm inward from the surface of the phantom (Fig. 2) [17]. T Five treatment plans were generated using the 2-field 3-dimentional conformal radiation therapy (2F-3DCRT), 4-field intensity-modulated radiation therapy (4F-IMRT), 7-field intensity-modulated radiation therapy (7F-IMRT), TomoHelical 3DCRT (TH-3DCRT), and TomoHelical intensity-modulated radiation therapy (TH-IMRT). he prescribed dose for the PTV was 200 cGy, which was equivalent to a single fraction dose. All treatment plans were created according to the recommendation of the Radiation Therapy Oncology Group guidelines. The PTV of 100 % of the prescribed dose represented ≥ 90 % of the minimum volume, and the total volume (normal tissue) of 30 % of the prescribed dose represented < 25 % of the maximum volume.

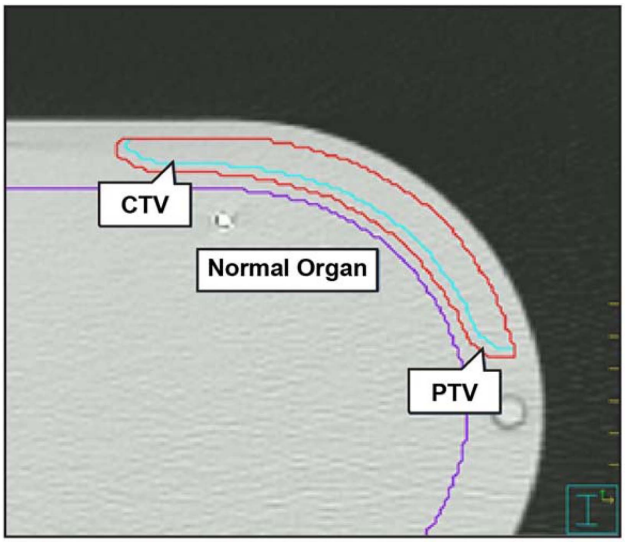

Fig. 2. (Color online) The phantom axial image, which displays the hypothetical target structures and the normal organ CTV, clinical target volume; PTV, planning target volume.

The 2F-3DCRT plan involved the application of the two-port tangential irradiation technique in the medial and lateral directions of the chest wall at gantry angles of 300° and 120°, respectively. The enhanced dynamic wedge filter was used for uniform dose distribution inside the PTV. For the 4F-IMRT and 7F-IMRT plans, an inverse plan was used, with gantry angles of 295°, 320°, 95°, and 125° for 4F-IMRT; and 295°, 320°, 350°, 30°, 70°, 100°, and 125° for 7F-IMRT for PTV optimization. For the TH-3DCRT and TH-IMRT treatment plans, the same radiation field width of 2.5 cm and pitch of 0.287 were used, whereas a modulation factor of 2.0 was used for TH-IMRT. The TH-3DCRT plan used the same two-port tangential irradiation technique in the medial and lateral directions of the chest wall at 300° and 120° angles, respectively, similar to that for the 2F-3DCRT plan.

2.3. Film dosimetry

The present study employed Gafchromic EBT3 film (ISP, International Specialty Products, Wayne, NJ, USA) to measure the 2-dimensional (2D) dose distribution in the chest wall. Gafchromic EBT3 film is designed measurement for absorbed dose of high-energy electromagnetic radiation such as gamma-ray and x-ray. The dynamic range of this film is designed for the best performance in the dose range 0.2 to 10Gy. Gafchromic EBT3 film doesn't need developing process and so it is also suitable for prompt and accurate dose measurement of high-energy electromagnetic radiation.

Gafchromic EBT3 film is composed of a water-equivalent material. It has often been used as a measurement tool for 2D dose distribution because of its low dependence on electromagnetic radiation energy in the megavoltage range, high spatial resolution, and it does not require a chemical image development process [18].

To evaluate the absorbed dose using Gafchromic EBT3, it is essential to obtain the dose-optical calibration curve. Pieces of the Gafchromic EBT3 film were placed in between each solid water phantom. The source to surface distance was set to 100 cm, and a radiation field of 5 × 5 cm^2 at a depth of 5 cm from the phantom surface was used. The high-energy electromagnetic beam of 6 MV from a linear accelerator was used to irradiate 20-320 cGy at intervals of 20 cGy each, and a dose analysis system was used to obtain the dose-optical calibration curve. The proper steps for assessing the Gafchromic EBT3 film were used, as described in the literature [19].

For the surface measurement, film cut at 3 × 25 cm^2 was tightly fixed onto the phantom surface. Both edges were fixed with tape, and analysis was conducted from the iso-center of the phantom to 16 cm, with the analyzed part divided into three regions: medial (0-40 mm), central (40-120 mm), and lateral (120-160 mm) (Fig. 3(a)).

To measure the superficial dose based on the phantom depth, 20 × 20 cm^2 film was inserted between the cross sections at the iso-center of the phantom and fixed as close as possible to the cross sections (Fig. 3(b)). Superficial parts of the phantom were divided into points of the three regions. Thus, before the measurement, the medial region (3 points), central region (4 points), and lateral region (3 points) connected to the iso-center were pre-marked at 15° intervals from 330-105°. The superficial dose was evaluated from 10 points at a depth of 1-6 mm.

In the present study, all measurements on the films were performed on the same day, and all measured films

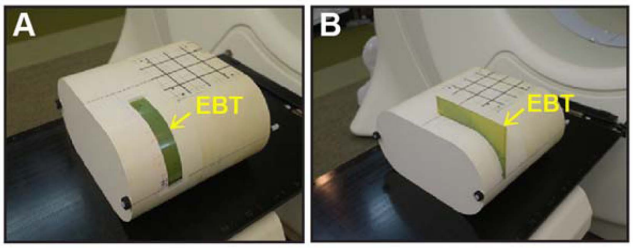

Fig. 3 (Color online) (a) EBT film strips (3 × 20 cm) were spread onto the phantom surface to measure the dose. Divided into three regions: medial (0-40 mm), central (40-120 mm), and lateral (120-160 mm). (b) EBT film pieces cut into 20 × 20 cm^2 squares were used to measure the doses inside the phantom.

were digitized using the VIDAR scanner (VXR-16 Dosimetry Pro, Vidar System Corporation, Herndon, VA, USA) within 24 hours of irradiation. Digitized measurement data were analyzed using a dose analysis system (RIT113 version 5.0, Radiological Imaging Technology, Colorado Springs, CO, USA).

2.4. Statistical analysis

Dose measurements using the Gafchromic EBT3 were affected by phantom set-up and treatment delivery precision; thus, measurements of the surface and superficial doses were performed up to three times each. Values are presented as average ± standard deviation and percentage of the prescribed dose. Measured doses were compared using the Student t-test and one-way analysis of variance. SPSS, version 17.0 (PASW, Chicago, IL, USA) was used to perform statistical analyses. P-values ≤ 0.05 were considered statistically significant.

3. Results

3.1. Surface dose

Analysis of the surface dose in the chest wall using Gafchromic EBT3 film showed that TH-3DCRT delivered 47-71% of the prescribed dose, which was the highest among all five treatment techniques. TH-IMRT, 2F-3DCRT, and 4F-IMRT delivered 43-55 %, 38-64 %, and 38-56 % of the prescribed dose, respectively, whereas 7F-IMRT delivered 35-46 % of the prescribed dose, the lowest measurement (Fig. 4).

The average surface doses are tabulated in Table 1. TH-3DCRT delivered 55.4 %, 64.4 %, and 52.0 % of the prescribed dose at the medial, central, and lateral regions, respectively, which represented the highest surface dose at each of the regions for all the treatment techniques. However, 7F-IMRT delivered 40.3 %, 43.3 %, and 43.2 % of the prescribed dose at the medial, central, and lateral regions, respectively, which represented the lowest surface doses on average.

In the case of 2F-3DCRT and TH-3DCRT, a significant increase in dose delivery of approximately 14 % and 9 % on average, respectively, was measured from the medial to central regions. Moreover, 4F-IMRT, 7F-IMRT, and TH-IMRT showed increases of dose delivery of approximately 6 %, 3 %, and 2 %, respectively, from the medial to central regions.

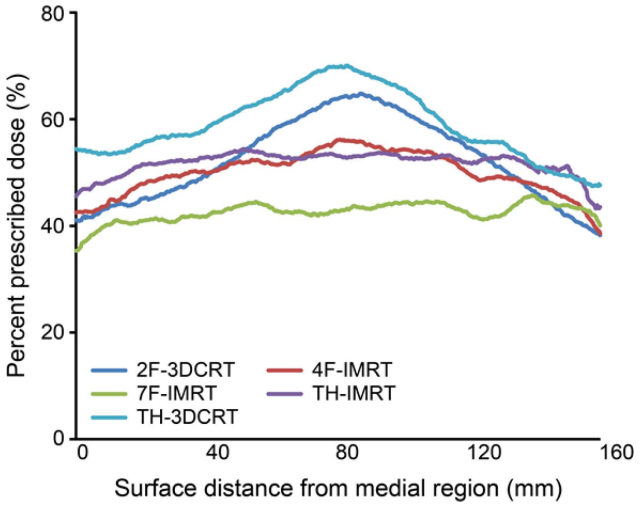

Fig. 4. (Color online) The surface dose measured with Gafchromic EBT3 film at various locations and different treatment techniques using high-energy electromagnetic radiation. The abscissa covers the distance in the iso-center plane from the medial field edge to the lateral field edge. The central region extends from 40 mm to 120 mm. 2F-3DCRT, 2-field 3-dimentional conformal radiation therapy; 4F-IMRT, 4-field intensity-modulated radiation therapy; 7F-IMRT, 7-field intensity-modulated radiation therapy; TH-3DCRT, TomoHelical 3DCRT; TH-IMRT, TomoHelical intensity-modulated radiation therapy.

3.2. Superficial dose

The average superficial doses are tabulated in Table 2. The superficial doses were ≥ 90 % of the prescribed dose at a depth of 6 mm in all the treatment techniques.

In the 2F-3DCRT plan, ≥ 65 % of the prescribed dose was delivered at a depth of 1 mm to the medial and lateral regions, whereas ≥ 70 % of the prescribed dose was delivered to the central region. At a depth of 2 mm, ≥ 70 % of the prescribed dose was delivered to the medial and

Table 1. Average surface dose for each region by the treatment technique

	2F-3DCRT	4F-IMRT	7F-IMRT	TH-IMRT	TH-3DCRT	*p*-value*
Medial	45.0 ± 1.0	46.8 ± 0.4	40.3 ± 0.6	50.1 ± 1.2	55.4 ± 0.2	< 0.001
Central	59.0 ± 0.7	53.2 ± 0.5	43.4 ± 0.7	53.1 ± 0.2	64.4 ± 0.3	< 0.001
Lateral	46.5 ± 0.7	46.6 ± 0.3	43.2 ± 0.7	50.4 ± 0.8	52.0 ± 0.3	< 0.001

Values are presented as percentages, i.e., relative to the prescribed dose. 2F-3DCRT, 2-field 3-dimentional conformal radiation therapy; 4F-IMRT, 4-field intensity-modulated radiation therapy; 7F-IMRT, 7-field intensity-modulated radiation therapy; TH-IMRT, TomoHelical IMRT; TH-3DCRT, TomoHelical 3DCRT.
*Based on analysis of variance.

Table 2 Average superficial dose for each region by the treatment technique

	2F-3DCRT	4F-IMRT	7F-IMRT	TH-IMRT	TH-3DCRT	p-value*
1 mm						
Medial	67.1 ± 0.4	66.9 ± 0.9	64.6 ± 0.6	75.5 ± 0.1	75.2 ± 0.1	< 0.001
Central	74.3 ± 0.9	76.4 ± 1.4	64.6 ± 1.3	75.5 ± 0.2	83.6 ± 2.0	0.004
Lateral	69.6 ± 0.9	67.7 ± 0.2	63.4 ± 0.7	75.3 ± 0.1	77.4 ± 0.3	< 0.001
2 mm						
Medial	76.2 ± 1.0	76.4 ± 0.6	76.2 ± 0.9	81.5 ± 0.3	81.0 ± 0.1	0.003
Central	84.1 ± 1.1	85.5 ± 1.7	75.1 ± 1.3	82.3 ± 0.5	91.9 ± 1.1	0.293
Lateral	78.5 ± 1.3	77.7 ± 0.5	73.5 ± 0.4	81.2 ± 0.6	83.9 ± 0.3	< 0.001
3 mm						
Medial	82.0 ± 1.3	82.6 ± 0.2	84.4 ± 1.0	86.3 ± 0.1	85.5 ± 0.9	0.006
Central	89.7 ± 1.4	91.0 ± 1.7	82.2 ± 1.7	87.0 ± 0.6	95.4 ± 1.3	0.581
Lateral	84.7 ± 1.6	85.3 ± 0.8	80.5 ± 0.5	85.0 ± 1.4	88.7 ± 0.6	0.014
4 mm						
Medial	85.9 ± 1.1	86.8 ± 0.3	89.7 ± 0.9	89.1 ± 0.5	89.0 ± 1.2	0.027
Central	93.0 ± 1.6	94.2 ± 1.5	86.9 ± 1.9	90.5 ± 0.7	96.9 ± 1.2	0.014
Lateral	90.2 ± 1.3	90.8 ± 1.6	86.3 ± 0.7	88.1 ± 1.8	92.0 ± 0.7	0.122
5 mm						
Medial	88.3 ± 0.8	89.1 ± 0.3	92.0 ± 1.0	91.0 ± 0.7	91.2 ± 1.3	0.087
Central	95.0 ± 1.6	95.4 ± 1.8	89.6 ± 2.0	92.4 ± 0.9	97.1 ± 1.2	0.025
Lateral	93.7 ± 1.3	94.7 ± 2.2	90.3 ± 0.7	91.1 ± 1.1	94.0 ± 0.5	0.022
6 mm						
Medial	90.5 ± 0.3	90.8 ± 0.2	93.5 ± 0.7	92.1 ± 0.6	91.7 ± 1.1	0.055
Central	96.0 ± 1.7	96.2 ± 2.0	91.6 ± 1.1	93.3 ± 0.9	97.3 ± 1.2	0.069
Lateral	96.7 ± 1.8	96.9 ± 2.6	92.8 ± 1.2	91.7 ± 1.5	95.7 ± 0.4	0.048

Values are presented as percentages, i.e., relative to the prescribed dose. 2F-3DCRT, 2-field 3-dimentional conformal radiation therapy; 4F-IMRT, 4-field intensity-modulated radiation therapy; 7F-IMRT, 7-field intensity-modulated radiation therapy; TH-IMRT, TomoHelical IMRT; TH-3DCRT, TomoHelical 3DCRT.
*Based on analysis of variance.

lateral regions, with 80 % of the prescribed dose received in the central region. At depths of 3-5 mm, ≥ 80 % of the prescribed dose was delivered to all the points, whereas ≥ 90 % of the prescribed dose was delivered at a depth of 6 mm. In the 4F-IMRT plan, ≥ 65 % of the prescribed dose was delivered at a depth of 1 mm to the medial and lateral regions, whereas ≥ 70 % of the prescribed dose was delivered to the central region. At a depth of 2 mm, the medial and central regions received ≥ 75 % of the prescribed dose, whereas at depths of 3 mm and 6 mm, all points received ≥ 80 % and 90 % of the prescribed dose, respectively. In the 7F-IMRT plan, the measured doses were similar to those of 4F-IMRT, and at depths of 1, 2, 4, and 6 mm from the surface, the measured doses were ≥ 60 %, 70 %, 80 %, and 90 % of the prescribed dose, respectively, representing uniform dose distribution in all the regions.

In the case of TH-IMRT and TH-3DCRT, ≥ 75 % of the prescribed dose was delivered to all the regions at a depth of 1 mm, whereas at depths of 2 mm and 5 mm, ≥ 80 % and 90 % of the prescribed doses were delivered, respectively. Similar to 7F-IMRT, TH-IMRT delivered a uniform dose to all regions. For TH-3DCRT, especially, the delivered dose was ≥ 80 % of the prescribed dose at a depth of 1 mm in the central region, and the superficial dose was ≥ 90 % of the prescribed dose at a depth of 2 mm.

4. Discussion

The present study measured and analyzed surface and superficial doses using several high-energy electromagnetic treatment techniques for PMRT. TH-3DCRT delivered the highest surface dose (47-71 % of the prescribed dose), whereas 7F-IMRT delivered the lowest dose; compared to that in the TH-3DCRT plan, the surface dose of 7F-IMRT decreased in all regions, by 15 % on average.

Previously, Quach et al. used Gafchromic EBT film, and they reported a surface dose from two-portal tangential irradiation that was similar to that in the present study

[20]. Moreover, studies by Yuichi Akino *et al.* and Almberg *et al.* also used the same technique to analyze comparative measurements between two-portal tangential irradiation and IMRT for the surface dose of the phantom on patients who had undergone partial mastectomy. Results from these studies showed that IMRT, with multiple irradiation beams (7-field), delivered a lower surface dose than the two-portal tangential irradiation technique, which was similar to the findings of the present study [21, 22].

For superficial dose measurements based on the depth of the phantom, TH-3DCRT and TH-IMRT delivered a dose of ≥ 75 % of the prescribed dose at a depth of 1 mm from the surface (Table 2). Generally, boluses are used for each organ to ensure that a sufficient dose is delivered to the skin and scar tissue of patients after postmastectomy. In the present study, tomotherapy, using 6 MV of electromagnetic beam energy, was able to deliver a sufficient dose of ≥ 75 % of the prescribed dose, which is the recommended dose, to the skin region at a depth of 1 mm without using a bolus. However, 7F-IMRT delivered a low dose of approximately 64 % of the prescribed dose at a depth of 1 mm. Therefore, the use of multiple irradiation beams such as IMRT can be expected to show a skin protection effect when the target is away from the skin at a set distance, especially when the skin does not contain any cancer cells.

As the chest wall of patients after postmastectomy is curved, the influence of the obliquity factor (OF) is present during tangential irradiation [23]. Due to the effect of OF on the surface dose, 2F-3DCRT, TH-3DCRT, and 4F-IMRT delivered an increased dose of approximately 14 %, 9 %, and 6 %, respectively, from the medial region to the lateral region, whereas 7F-IMRT and TH-IMRT showed uniform doses of approximately 3 % and 2%, respectively. Regarding a superficial dose based on depth, 4F-IMRT, 2F-3DCRT, and TH-3DCRT, which used tangential irradiation, delivered a higher average dose to the central region than to the medial or lateral region, and TH-3DCRT in particular delivered very high superficial doses of ≥ 80 % and ≥ 90 % of the prescribed dose at depths of 1 mm and 2 mm, respectively. However, 7F-IMRT and TH-IMRT delivered a uniform dose at each depth, similar to the results of the surface dose measurement. Therefore, it was determined that as the irradiation beam moves toward the central region, it affects the OF.

5. Conclusions

When using the bolus application, one has to consider the possible skin reactions of PMRT with high-energy electromagnetic beam. In the present study, TH-3DCRT and TH-IMRT delivered higher surface and superficial doses than LINAC based treatment techniques. If the superficial region is a high-risk area at a depth of 1 mm from the surface in the chest wall, TH-3DCRT and TH-IMRT can provide a sufficient dose of 75.2-83.6 %, 75.3-75.5 % of the prescribed dose (i.e., the recommended dose), respectively. It can prevent skin reactions, as a bolus is unnecessary. Furthermore, because the absorbed dose in the skin region is affected by the treatment technique and the incident angle of irradiation when treating curved regions with a thin tissue layer such as the chest wall, an appropriate treatment technique is necessary.

References

[1] T. J. Whelan, J. Julian, J. Wright, A. R. Jadad, and M. L. Levine, J. Clin. Oncol. **18**, 1220 (2000).
[2] M. Clarke, R. Collins, S. Darby, C. Davies, P. Elphinstone, V. Evans, J. Godwin, R. Gray, C. Hicks, S. James, E. MacKinnon, P. McGale, T. McHugh, R. Peto, C. Taylor, and Y. Wang; Early Breast Cancer Trialists' Collaborative Group (EBCTCG). Lancet. **366**, 2087 (2005). [DOI]: 10.1016/S0140-6736(05)67887-7
[3] International Commission on Radiological Protection (ICRP), The Biological Basis for Dose Limitation in the Skin. ICRP Skin Task Group Report, ICRP Publication 59. Annals of the ICRP 22(2). (1992). [DOI]: 10.1016/0146-6453(91)90039-J
[4] J. O. Archambeau, R. Pezner, and T. Wasserman, Int. J. Radiat. Oncol. Biol. Phys. **31**, 1171 (1995). [DOI]: 10.1016/0360-3016(94)00423-I
[5] K. S. C. Chao, C. A. Perez, and L. W. Brady, Radiation Oncology Management Decisions, 3rd ed. Lippincott Williams & Wilkins, Philadelphia (2002) pp 367-375.
[6] T. R. Mackie, T. Holmes, and S. Swerdloff, Med. Phys. **20**, 1709 (1993).
[7] G. M. Uschold, Principles and Practice of Radiation Therapy, 2nd ed. C.V. Mosby, St. Louis (2004) pp 843-874.
[8] T. T. Vu, J. P. Pignol, E. Rakovitch, J. Spayne, and L. Paszat, Clin. Oncol. (R Coll Radiol) **19**, 115 (2007). [DOI]:10.1016/j.clon.2006.10.004
[9] B. Yang, X. D. Wei, Y. T. Zhao, and C. M. Ma, Med. Dosim. **39**, 185 (2014). [DOI]: 10.1016/j.meddos.2013
[10] E. A. Krueger, B. A. Fraass, D. L. McShan, R. Marsh, and L. J. Pierce, Int. J. Radiat. Oncol. Biol. Phys. **56**, 1023 (2003). [DOI]: http://dx.doi.org/10.1016/S0360-3016(03)00183-4
[11] K. Tournel, D. Verellen, M. Duchateau, Y. Fierens, N. Linthout, T. Reynders, M. Voordeckers, and G. Storme, Radiother. Oncol. **84**, 34 (2007). [DOI]: 10.1016/j.radonc.2007.06.003
[12] K. S. Smith, J. P. Gibbons, B. J. Gerbi, and K. R. Hog-

strom, Med. Phys. **35**, 769 (2008). [DOI]: 10.1118/1.2828206
[13] N. de la Torre, C. T. Figueroa, K. Martinez, S. Riley, and J. Chapman, Med. Dosim. **29**, 109 (2004). [DOI]: 10.1016/j.meddos.2004.03.002
[14] V. Panettieri, P. Barsoum, M. Westermark, L. Brualla, and I. Lax, Radiother. Oncol. **93**, 94 (2009). [DOI]: 10.1016/j.radonc.2009.05.010
[15] A. C. Shiau, M. C. Chiu, T. H. Chen, J. F. Chiou, P. W. Shueng, S. W. Chen, W. L. Chen, and W. P. Kuan, Med. Dosim. **37**, 417 (2012). [DOI]: 10.1016/j.meddos.2012.03.005
[16] F. M. Khan, The Physics of Radiation Therapy, 5rd edn, Lippincott Williams & Wilkins, Philadelphia (2014) pp. 9.
[17] L. Hong, M. Hunt, C. Chui, S. Spirou, K. Forster, H. Lee, J. Yahalom, G. J. Kutcher, and B. McCormick, Int. J. Radiat. Oncol. Biol. Phys. **44**, 1155 (1999). [DOI]: http://dx.doi.org/10.1016/S0360-3016(99)00132-7
[18] M. Fuss, E. Sturtewagen, C. De Wagter, and D. Georg, Phys. Med. Biol. **52**, 4211 (2007). [DOI]: 10.1088/0031-9155/52/14/013
[19] M. J. Butson, J. N. Mathur, and P. E. Metcalfe, Phys. Med. Biol. **41**, 1073 (1996). [DOI]: 10.1088/0031-9155/41/6/011
[20] K. Y. Quach, J. Morales, M. J. Butson, A. B. Rosenfeld, and P. E. Metcalfe, Med. Phys. **27**, 1676 (2000). [DOI]: 10.1118/1.599035
[21] Y. Akino, I. J. Das, G. K. Bartlett, H. Zhang, E. Thompson, and J. E. Zook, Med. Phys. **40**, 011714 (2013). [DOI]: 10.1118/1.4770285
[22] S. Almberg, T. Lindmo, and J. Frengen, Radiother. Oncol. **100**, 259 (2011). [DOI]: 10.1016/j.radonc.2011.05.021
[23] B. J. Gerbi, A. S. Meigooni, and F. M. Khan, Med. Phys. **14**, 393 (1987). [DOI]: 10.1118/1.596055